8-27-2012

Control of reflectance and transmittance in scattering and curvilinear hyperbolic metamaterials

T. U. Tumkur
Norfolk State University

J. K. Kitur
Norfolk State University

B. Chu
Norfolk State University; Cornell University

Lei Gu
Norfolk State University

V. A. Podolskiy
University of Massachusetts Lowell

See next page for additional authors

Authors
T. U. Tumkur, J. K. Kitur, B. Chu, Lei Gu, V. A. Podolskiy, Evgenii E. Narimanov, and M. A. Noginov

AIP Applied Physics Letters

Control of reflectance and transmittance in scattering and curvilinear hyperbolic metamaterials

T. U. Tumkur, J. K. Kitur, B. Chu, Lei Gu, V. A. Podolskiy et al.

Citation: Appl. Phys. Lett. 101, 091105 (2012); doi: 10.1063/1.4746387
View online: http://dx.doi.org/10.1063/1.4746387
View Table of Contents: http://apl.aip.org/resource/1/APPLAB/v101/i9
Published by the AIP Publishing LLC.

Control of reflectance and transmittance in scattering and curvilinear hyperbolic metamaterials

T. U. Tumkur,[1] J. K. Kitur,[1] B. Chu,[2,3] Lei Gu,[1] V. A. Podolskiy,[4] E. E. Narimanov,[5] and M. A. Noginov[1,a)]
[1]*Center for Materials Research, Norfolk State University, Norfolk, Virginia 23504, USA*
[2]*Summer Research Program, Center for Materials Research, Norfolk State University, Norfolk, Virginia 23504, USA*
[3]*Materials Science and Engineering, Cornell University, Ithaca, New York 14853, USA*
[4]*Department of Physics and Applied Physics, University of Massachusetts Lowell, Lowell, Massachusetts 01854, USA*
[5]*Birck Nanotechnology Center, Purdue University, West Lafayette, Indiana 47907, USA*

(Received 21 June 2012; accepted 1 August 2012; published online 27 August 2012)

We demonstrate reduced reflectance in curvilinear lamellar hyperbolic metamaterials as well as planar hyperbolic metamaterials consisting of metal/dielectric multilayers, with scatterers deposited on the top. The reduced reflectance is accompanied by a significant enhancement in transmission along with non-reciprocity of transmittance in forward and backward propagating directions. The observed experimental behavior is qualitatively similar to the results of numerical solutions of Maxwell equations. The findings of this study pave the way to a variety of important applications, including broadband enhancement of light trapping in photovoltaic devices. © *2012 American Institute of Physics*. [http://dx.doi.org/10.1063/1.4746387]

Engineered composite materials with sub-wavelength inclusions, or metamaterials, have received widespread attention due to their ability to manipulate light in unconventional ways, as exemplified by negative index of refraction,[1–3] optical cloaking,[4,5] and limitless focusing.[6,7] Hyperbolic metamaterials, also known as indefinite media,[8] is an important class of metamaterials, in which dielectric permittivities in orthogonal directions have opposite signs.[8–11] This property, leading to a hyperbolic dispersion,[12] enables propagation of waves with nominally infinitely large wavevectors (which extend to vacuum as evanescently decaying "tails"), and infinite density of photonic states.[13] Metamaterials with hyperbolic dispersion support and facilitate scores of unparalleled phenomena including, but not limited to sub-diffraction imaging,[12,14,15] control of spontaneous emission,[16–19] and perfect absorption.[20]

In this work, we report on the reduction of reflectance from hyperbolic metamaterials, enabled by their curvilinear shapes as well as scatterers placed on their surface. The reduced reflectance is accompanied by an enhancement in transmission along with non-reciprocity of transmittance in forward and backward propagation directions.

The origin of the reduced reflectance can be understood in terms of the Fermi's golden rule, which predicts that the rate of a transition and, correspondingly, the rate and the directionality of light scattering are determined by the density of photonic states in the surrounding medium.[20] If a small scatterer is placed in the vicinity (of the order of several tens of nanometers) of a hyperbolic metamaterial, an incident light will be scattered preferentially *inside* the medium, resulting in suppressed reflectance and diffuse scattering. However, a dilemma exists. If the scatterers deposited on a plane hyperbolic metamaterial are small, they do not scatter light efficiently; and if they are large, they are not within the range of the metamaterial's high density of states, and the scattering *inside* the metamaterial is weak again. Therefore, enabled by scatterers, reduction of reflectance in a plane lamellar metal-dielectric metamaterial is expected to be modest. Note that due to small thicknesses of lamellar hyperbolic metamaterials ($\leq 1\ \mu$m),[17–19] roughening of their surfaces by grinding, which was implemented in thick alumina membranes,[20] is not practical. Intuitively, a much stronger reduction of reflection is predicted if a multilayered metamaterial with hyperbolic dispersion is deposited on a roughened surface or an array of scatterers.

In our studies, in the first series of experimental samples, alternating layers of Ag and MgF_2 were evaporated onto flat glass substrates. The structures consisted of 14 layers (7 periods) of Ag and MgF_2 films with the thicknesses 25 nm and 35 nm, respectively. The thickness measurements were done using a DekTak-6 profilometer. The fabricated multilayered metamaterials had hyperbolic dispersion (characterized by negative dielectric permittivity in the direction parallel to the layers and positive dielectric permittivity in the direction perpendicular to the layers) at $\lambda \geq 360$ nm.[19] Titanium dioxide (TiO_2) nanopowder with a mean particle size of $\sim$330 nm (obtained from DuPont) was suspended in dichloromethane (DCM), in concentration 7 mg/mL, and deposited drop by drop onto lamellar metamaterial, silver, and glass substrates, which were preheated to $\sim$70 °C. After drying, the suspensions resulted in mono- and multi-layers of TiO_2 nanoparticles of varying filling factors.

In preparation of the second series of samples, an aqueous suspension of glass microspheres (11.6 mg/mL) was added (in the form of droplets) onto glass substrates, which were preheated to $\sim$130 °C. The diameters of glass microspheres ranged from 2 to 10 μm. After drying, microspheres formed monolayers (with high filling factor of $\sim$80%) and occasionally double-layers of particles. A half of each

[a)]Author to whom correspondence should be addressed. Electronic mail: mnoginov@nsu.edu.

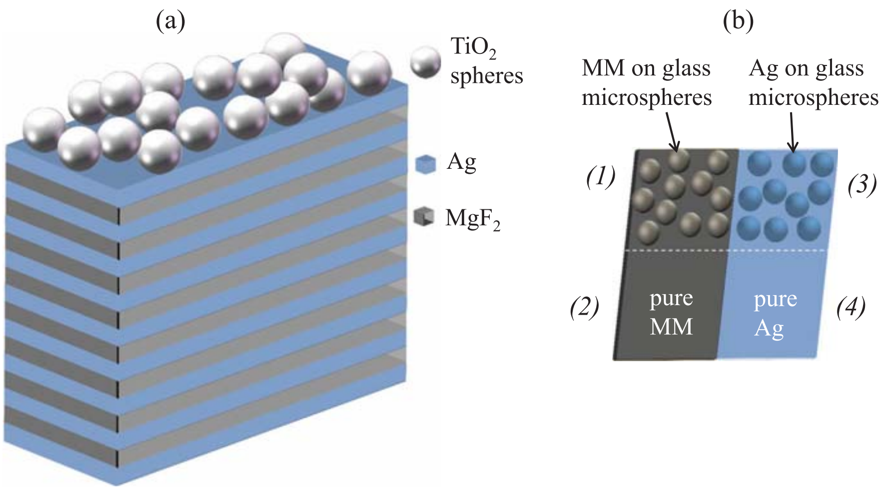

FIG. 1. (a) Schematic of a lamellar Ag/MgF_2 hyperbolic metamaterial used in the experiments (Ag ~25 nm, MgF_2 ~35 nm), with 330 nm TiO_2 nanoparticles deposited on the top. (b) Schematic of a microsphere-based sample containing four principle areas: (1) multilayered metamaterial on top of microspheres, (2) multilayered metamaterial on top of glass, (3) silver on top of microspheres, and (4) silver on top of glass.

sample was covered with Ag/MgF_2 multilayers (three periods or six periods in different experiments), while the other half was covered with ~200 nm Ag film. Silver and Ag/MgF_2 multilayers were also deposited on top of the same glass substrates without glass microspheres. Thus, each sample had four areas: Ag/MgF_2 metamaterial on microspheres, Ag/MgF_2 metamaterial on glass, Ag film on microspheres, and Ag film on glass (Fig. 1(b)).

The transmittance and reflectance of all samples were measured using a Lambda 900 UV-vis-IR spectrophotometer equipped with an integrating sphere, at both front (side of scatterers or coated microspheres) and back (rear side of a glass substrate) illumination.

With increase of concentration of TiO_2 nanoparticles on top of flat metamaterials samples, the reflectance initially decreased, from ~90% to ~65% (Fig. 2(a)), and then increased again at even higher nanoparticle concentrations (inset of Fig. 2(a)). This behavior is easy to understand qualitatively. In fact, at small nanoparticle concentrations, not the whole area of the sample is covered, and the reduction of reflectance is modest. At higher concentration, corresponding to approximately full coverage of a metamaterial with one layer of nanoparticles, the scattering is stronger and the reduction of reflectance is maximal. However, at even larger concentrations of nanoparticles, they form multiple layers, and a significant fraction of photons is scattered back before reaching the metamaterial's surface. Unsurprisingly, this leads to an increase of the sample's diffused reflectance.

The same nanoparticles were also deposited on a ~200 nm silver film, but its reflectance reduced only by ~5%—the effect partly caused by scattering to evanescent modes of the metal (Fig. 2(a)). One should note that modest reduction in reflectance off a hyperbolic metamaterial with deposited TiO_2 nanoparticles was accompanied by a stronger (nearly twofold) enhancement of transmittance, measured in 2π solid angle at front illumination (from the side of nanoparticles), Fig. 2(b). The metamaterial's reflectance at rear illumination was comparable to that of a pure sample (without nanoparticles). Correspondingly, scatterers caused nonreciprocity of the sample's transmittance in forward and backward directions, Fig. 2(b). (This effect is possible in a system with scatterers, which randomly change directions of photon propagation.)

The reflectance and transmittance of metamaterials samples was modeled using COMSOL Multiphysics solver. Figure 3(a) shows the distribution of the absolute value of electric field (color-coded map as well as profile on the right) at excitation of a planar multilayered Ag/MgF_2 metamaterial from

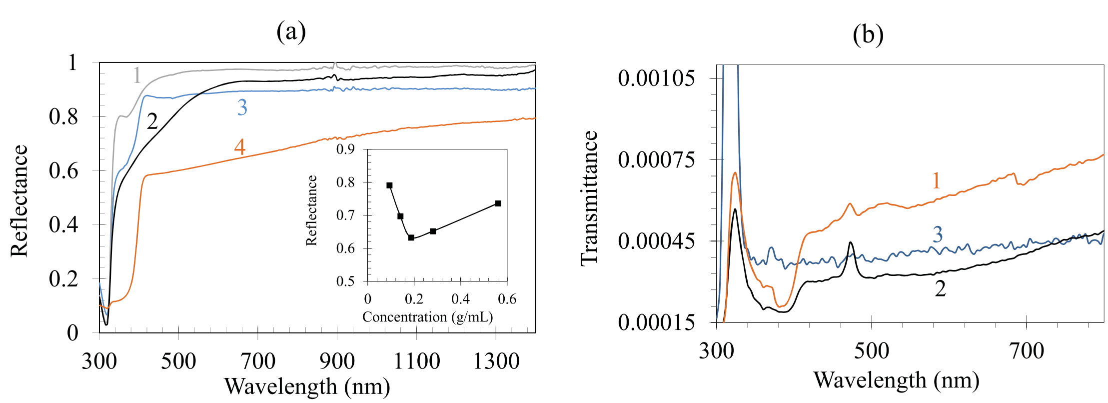

FIG. 2. (a) Reflectance spectra (at front illumination) of a silver film (trace 1), pure lamellar Ag/MgF_2 metamaterial (15 layers, top layer is silver, trace 2), silver film with deposited TiO_2 nanoparticles (trace 3), and lamellar metamaterial with TiO_2 nanoparticles (trace 4). Inset: Dependence of reflectance of a lamellar hyperbolic metamaterial (at $\lambda = 550$ nm) as a function of concentration of TiO_2 nanoparticles. (b) Transmittance spectra of a lamellar metamaterial sample with deposited TiO_2 nanoparticles, illuminated from the side of nanoparticles (trace 1) and from the side of substrate (trace 2). Trace 3—transmission spectrum of the metamaterial without nanoparticles.

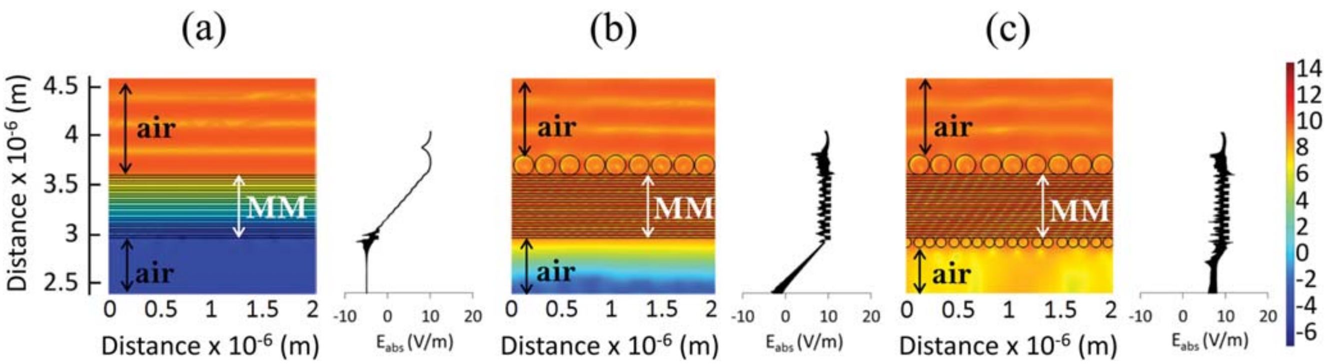

FIG. 3. Absolute value of electric field (defined as $E_{abs} = \sqrt{|E_x|^2 + |E_y|^2}$) in (a) a pure Ag/$MgF_2$ metamaterial (Ag on the top and at the bottom); (b) same as in (a), with 200 nm TiO_2 spheres placed on the top (with ~88% linear coverage); and (c) same as in (b), with 100 nm spheres attached to the bottom. The metamaterial consisted of eleven Ag layers (25 nm) and 10 MgF_2 layers (35 nm). The color bar shows natural logarithmic color coding. The same electric field distributions are plotted on the right of each color map. (The lines depict the spread of intensities at each (vertical) distance positions, which gives them a noisy appearance.)

the top at 8° incidence angle. One can see that light penetrates into a metamaterial as an evanescent wave, with characteristic (intensity) skin depth equal to ~23 nm. If a layer of 200 nm spherical TiO_2 nanoparticles is deposited on the top of a metamaterial, light, following the Fermi's golden rule, is efficiently scattered *inside* the medium. However, traveling waves do not come out from the sample through the opposite flat side. Instead, only exponentially decaying electric field intensity (with characteristic decay length ~21 nm) is found on the back, Fig. 3(b). The situation changes radically if an extra layer of spherical 100 nm TiO_2 nanoparticles is added to the rear side of the metamaterial, Fig. 3(c). In this case, nanoparticles on the front of the sample let light to enter the metamaterial, while nanoparticles on the back let travelling waves to couple out with appreciable transmission efficiency. (In the 2D COMSOL simulation, nominally spherical TiO_2 nanoparticles were modeled as cylinders. For the consistency of presentation, we refer to them as spheres.)

The calculated specular reflectance spectra of the pure metamaterial and the metamaterial with 200 nm nanoparticles on the top are shown in Fig. 4(a) (traces 1 and 2). One can see that addition of nanoparticles strongly reduces the sample's reflectance, in a qualitative agreement with the experiment. Scatterers added to the bottom of the metamaterial (100 nm TiO_2 nanoparticles) do not change the reflectance significantly (Fig. 4(a), trace 3). At the same time, shapes of the reflectance spectra are highly sensitive to the sizes of nanospheres on the top of the sample (compare traces 3 and 4 in Figure 4(a)).

Shapes of multi-spiked reflectance spectra are determined by resonances of hybridized nanosphere/metamaterial modes. We infer that in experimental samples, size dispersion (ranging from 200 to 400 nm), not ideal spherical shapes, and strong coupling of touching each other nanoparticles smeared sharp features, resulting in nearly flat spectra of Fig. 2(a).

The calculated transmittance of a pure metamaterial, metamaterial with 200 nm TiO_2 nanoparticles on the front and 100 nm nanoparticles in the rear, illuminated from the front, and the same metamaterial illuminated from the rear are shown in Fig. 4(b). One can see that in agreement with experiments, the transmittance of a pure metamaterial, which is practically zero in the visible and infrared parts of the spectrum, increases significantly with addition of nanoparticles. The calculation also predicts non-reciprocity of transmission, which details depend on the wavelength and strengths of scattering centers on both sides of the metamaterial.

The fact that an appreciable transmittance (much larger than that predicted by COMSOL simulations, Fig. 4) was experimentally observed even in the metamaterial samples without

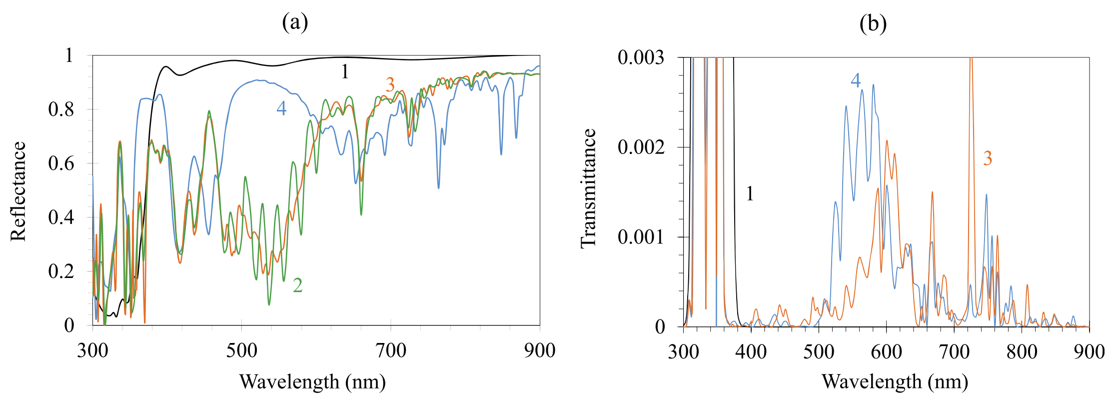

FIG. 4. (a) Calculated reflectance spectra of a lamellar Ag/MgF_2 metamaterial with no nanoparticles (trace 1), with 200 nm TiO_2 nanoparticles on the top (trace 2), with 200 nm nanoparticles on the top and 100 nm nanoparticles at the bottom (trace 3), and with 100 nm nanoparticles on the top and 200 nm nanoparticles at the bottom (trace 4). (b) Calculated transmission spectra of the samples 1, 3, and 4 from (a).

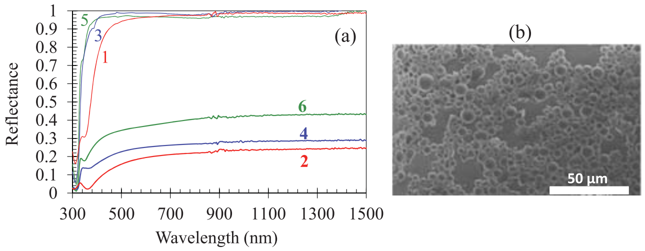

FIG. 5. (a) Reflectance spectra (front illumination) of a metamaterial consisting of three pairs of Ag/MgF_2 layers, deposited on a flat substrate (trace 1), and on glass microspheres (trace 2). Traces 3 and 4—same for a metamaterial consisting of six pairs of Ag/Mg_2 layers. Traces 5 and 6—same for a silver film. (b) Scanning electron microscope (SEM) image of a lamellar metamaterial deposited onto glass microspheres.

deposited nanoparticles can be explained by unintentional roughness (r.m.s. $\approx$ 2.5 nm) and inhomogeneities of the metamaterials' layers. As noted above, because of not complete correspondence of the experiment and the simplified model assumptions, the agreement between the model and the experiment could be only qualitative but not quantitative.

A significantly stronger reduction of reflectance was observed in a metamaterial deposited onto glass microspheres, Figs. 5(a) and 5(b). For a "front" side illumination (the side of deposited metamaterial), a slightly stronger effect (reduction down to ~18%) was observed in a thin metamaterial consisting of three pairs of Ag/MgF_2 layers rather than in a thicker metamaterial consisting of six pairs of Ag/MgF_2 layers, Fig. 5(a). Comparable results have been observed at the "back" side illumination (the side of glass substrate), although in this case a stronger reduction of reflectance was observed in the metamaterial consisting of six Ag/MgF_2 layers. Note that a substantial (down to ~35%) reduction of reflectance was observed when a ~200 nm silver film was deposited on similar microspheres. This effect could be partly caused by the sample's transmittance and partly by coupling light to evanescent lossy modes of silver.

We, thus, have demonstrated the predicted reduction of reflectance in lamellar hyperbolic metamaterials. The effect was stronger in curvilinear structures than in plane multilayered samples with deposited TiO_2 scatterers. The reduction of reflectance was accompanied by a significant enhancement of transmittance and non-reciprocity of the samples' transmission in forward and backward directions. The results of COMSOL simulations were consistent with the observed reduction in reflectance (in a flat hyperbolic metamaterial with deposited TiO_2 nanoparticles) and also confirmed the effect of non-reciprocity in transmission. The observed results pave the way for a variety of unparalleled applications including broadband enhancement of light trapping in photovoltaic devices.

The work was partly supported by the NSF Grant No. DMR 1205457, NSF PREM Grant No. DMR 0611430, NSF NCN Grant No. EEC-0228390, NSF Grant No. ECCS-110283, AFOSR Grant No. FA9550-09-1-0456, NSF IGERT Grant No. DGE 0966188, UTC #10-S567-001502C4, W911NF-07-1-0343, and 50342-PH-MUR.

[1]R. Shelby, D. R. Smith, and S. Schultz, Science **292**, 77 (2001).
[2]D. R. Smith, J. B. Pendry, and M. C. K. Wiltshire, Science **305**, 788 (2004).
[3]S. Zhang, W. Fan, N. C. Panoiu, K. J. Malloy, R. M. Osgood, and S. R. J. Brueck, Phys. Rev. Lett. **95**, 137404 (2005).
[4]J. B. Pendry, D. Schurig, and D. R. Smith, Science **312**, 1780 (2006).
[5]U. Leonhardt, Science **312**, 1777 (2006).
[6]J. B. Pendry, Phys. Rev. Lett. **85**, 3966–3969 (2000).
[7]G. V. Eleftheriades, A. K. Iyer, and P. C. Kremer, IEEE Trans. Microwave Theory Tech. **50**, 2702 (2002)
[8]D. R. Smith and D. Schurig, Phys. Rev. Lett. **90**, 077405 (2003).
[9]C. R. Simovski and P. A. Belov, Phys. Rev. E **70**, 046616 (2004).
[10]A. J. Hoffman, L. Alekseyev, S. S. Howard, K. J. Franz, D. Wasserman, V. A. Podolskiy, E. E. Narimanov, D. L. Sivco, and C. Gmachl, Nature Mater. **6**, 946 (2007).
[11]M. A. Noginov, Yu. A. Barnakov, G. Zhu, T. Tumkur, H. Li, and E. E. Narimanov, Appl. Phys. Lett. **94**, 151105 (2009).
[12]Z. Jacob, L. V. Alekseyev, and E. Narimanov, Opt. Exp. **14**, 8247 (2006).
[13]Z. Jacob, I. I. Smolyaninov, and E. E. Narimanov, Appl. Phys. Lett. **100**, 181105 (2012).
[14]A. Salandrino and N. Engheta, Phys. Rev. B **74**, 075103 (2006).
[15]J. Yao, Z. Liu, Y. Liu, Y. Wang, C. Sun, G. Bartal, A. Stacy, and X. Zhang, Science **321**, 930 (2008).
[16]M. A. Noginov, H. Li, Y. A. Barnakov, D. Dryden, G. Nataraj, G. Zhu, C. E. Bonner, M. Mayy, Z. Jacob, and E. E. Narimanov, Opt. Lett. **35**(11), 1863–1865 (2010).
[17]Z. Jacob, J. Kim, G. V. Naik, A. Boltasseva, E. E. Narimanov, and V. M. Shalaev, Appl. Phys. B **100**, 215–218 (2010).
[18]H. N. S. Krishnamoorthy, Z. Jacob, E. E. Narimanov, I. Kretzchmar, and V. M. Menon, Science **336**, 205 (2012).
[19]T. Tumkur, G. Zhu, P. Black, Yu. A. Barnakov, C. E. Bonner, and M. A. Noginov, Appl. Phys. Lett. **99**, 151115 (2011).
[20]E. E. Narimanov, H. Li, Yu. A. Barnakov, T. U. Tumkur, and M. A. Noginov, e-print arXiv:1109.5469.